

SYNTHESIS AND ELECTRICAL PROPERTIES OF $\text{Sr}_3\text{NiNb}_2\text{O}_9$ – MATERIALS FOR SOFCs

Q. LI *, Z. P. LIU, R. YAN, L. M. DONG

College of Materials Science and Engineering, Harbin University of Science & Technology Harbin, China

Perovskite-based anodes for Solid Oxide Fuel Cells (SOFCs) have received attention in recent years due to mixed ionic and electronic conductivity and good properties. This paper presents the synthesis and electrical conductivity of $\text{Sr}_3\text{NiNb}_2\text{O}_9$ -based compounds. $\text{Sr}_3\text{NiNb}_2\text{O}_9$ -based compounds were synthesized using a conventional solid-state reaction in air. The structure of perovskite-related compounds with the composition of $\text{Sr}_3\text{Ni}_{1+x}\text{Nb}_{2-x}\text{O}_9$ ($0 \leq x \leq 1$) was evaluated analyzing the evolution with composition of the X-ray diffraction patterns (PXRD). The pure $\text{SrNi}_{0.33}\text{Nb}_{0.67}\text{O}_3$ phase (JCPDS: 17-0179) was found for $\text{Sr}_3\text{Ni}_{1+x}\text{Nb}_{2-x}\text{O}_9$ ($0 \leq x \leq 0.25$). With the increase of Ni content, the second phase NiO appeared. The Electrical conductivity of $\text{Sr}_3\text{NiNb}_2\text{O}_9$ in air, H_2 and wet H_2 atmospheres from 300°C to 800°C by subsequent heating and cooling cycles was determined by AC impedance using Pt electrodes. The spectra show somewhat depressed arcs. The contributions due to bulk (b), grain-boundary (gb), and electrode (e) effects were observed at high, intermediate and low-frequency regions, especially at low temperatures. The electrical conductivity of the $\text{Sr}_3\text{NiNb}_2\text{O}_9$ compounds was found to vary in different atmospheres (air, H_2 and wet H_2). The electrical conductivity increases in H_2 compared to air. In H_2 , the $\text{Sr}_3\text{NiNb}_2\text{O}_9$ compounds exhibit $2.22 \times 10^{-3} \text{ S}\cdot\text{cm}^{-1}$ at 625°C , which is about four orders of magnitude higher than that in air. The activation energy was found to be 1.17 eV, 0.72 eV, 0.83 eV in air, dry H_2 and wet H_2 respectively.

(Received February 17, 2016; Accepted April 4, 2016)

Keywords: $\text{Sr}_3\text{Ni}_{1+x}\text{Nb}_{2-x}\text{O}_9$. Electrical properties. SOFC anodes. AC Impedance. Perovskite

1. Introduction

Conversion of chemical energy into electrical energy became more important due to the increase in the use of electricity. Fuel cells, especially, solid oxide fuel cell (SOFC) may well be an option for future power generation because of their modular and distributed nature, zero noise pollution, and low levels of emissions, greenhouse gases, and toxic gases [1]. SOFC is an electrochemical cell which converts directly chemical reaction energy into electrical energy and heat. Typically, it consists of an oxide ion electrolyte and mixed ionic and electronic conducting electrodes (cathode and anode). Currently, there is a great deal of interests in the development of both oxide ion electrolytes and electrodes for application to advanced intermediate temperature (IT) SOFCs as well as for gas sensors (e.g., O_2 , hydrocarbons, H_2) [2- 8]. To date, commercial SOFC materials are the Y_2O_3 -doped ZrO_2 (YSZ) electrolyte, Sr-doped LaMnO_3 (LSM) cathode, Ni + YSZ cermet composite anode and Sr-doped LaCrO_3 interconnector. [9-14]

*Corresponding author:qinalily@163.com.

There are commonly two approaches that were adopted in the development of SOFC anode materials. The first approach involves conventional metal and solid electrolyte composites and the second method utilizes ionic and electronic conducting single phase compounds. In the former type, the electronic conductivity is controlled by the metal and the ionic conductivity is provided by electrolytes. While in the second type, both ionic and electronic conductivity are controlled by a single compound. The later approach overcomes several materials challenges but none of the anode materials can meet simultaneously all these properties requirements, hence research is being focused now to improve the functional properties of metal oxide anodes possessing perovskite, perovskite-related double and layered (2D) perovskites, fluorites, and pyrochlores structures by chemical doping and synthesis methods.[12,15-17]

Among the various known mixed conducting anodes, perovskite and fluorite- type anode materials are drawn attention because of their superior chemical stability in S and CO containing fuels environment and also excellent catalytic activity. Recently Goodenough's group reported double perovskite-related structure $\text{Sr}_2\text{MgMoO}_6$ as anode materials for advanced SOFCs [18]. $\text{Sr}_2\text{MgMoO}_{6-\delta}$ and $\text{Sr}_2\text{MnMoO}_{6-\delta}$ under the reducing atmosphere at an anode showed loss of oxygen with retention of the double-perovskite structure. Their electronic conductivities in an atmosphere of H_2 and CH_4 were about $10 \text{ S}\cdot\text{cm}^{-1}$ at $800 \text{ }^\circ\text{C}$. These double perovskites exhibit good chemical stability in H_2S and show a superior single-cell performance in hydrogen and methane. In this paper, we report a new series of Mo-doped $\text{Sr}_3\text{Ni}_{1+x}\text{Nb}_{2-x}\text{O}_{9-\delta}$ ($0 \leq x \leq 1$) (SNNO) as potential anodes materials for application in IT-SOFCs. The conductivity in different atmosphere was measured for $\text{Sr}_3\text{NiNb}_2\text{O}_9$.

2. Materials and methods

2.1. Materials Preparation

$\text{Sr}_3\text{Ni}_{1+x}\text{Nb}_{2-x}\text{O}_{9-\delta}$ ($0 \leq x \leq 1$) (SNNO) were prepared by a conventional solid-state reaction in air using stoichiometric amounts of high purity SrCO_3 (>99.9%, Alfa Aesar), NiO (>99.5%, Alfa Aesar) and Nb_2O_5 (>99.5%, Alfa Aesar). The powders were mixed using a ball mill (Pulverisette, Fritsch, Germany) for 6 h at 200 rpm using zirconia balls and 2-propanol. The mixed powders were then dried and heated in air at $1000 \text{ }^\circ\text{C}$ for 12 h in a clean alumina crucible. The resulting mixture was ball-milled using 2-propanol again for about 6 h and then pressed into pellets (~1 cm diameter and ~2 cm length) using an isostatic pressure. The pressed green pellets were sintered in air at $1400 \text{ }^\circ\text{C}$ for 24 h twice and then $1450 \text{ }^\circ\text{C}$ for 24 h twice, with repeated mixing procedures at each step. The pellets were then ball milled for powder X-ray diffraction (PXRD) characterization using a Rigaku powder X-ray diffractometer (Cu $K\alpha$, 40 kV, 40 mA) (Cu $K\alpha$, 40 kV, 40 mA) at room temperature with a 2θ step scan width of 0.02° and a counting time of 6 s. The lattice constant was determined from the PXRD data by least-squares refinement.

2.2. Electrical Characterization

Electrical conductivity measurements were performed on sintered pellets (~0.15 cm in thickness, ~1 cm in diameter) in air, dry H_2 , wet H_2 using Pt electrodes. Pt paste (LP A88-11S, Heraeus Inc., Germany) was applied using a paint brush to both sides of the sintered pellets and cured at $800 \text{ }^\circ\text{C}$ for 1 h in air to remove the organic binders. Pt wires were attached to the surface of the pellet using a spring-loaded contact, which served as a current collector. The cell was heated to the desired temperature in the range of $300\text{-}800 \text{ }^\circ\text{C}$ using a Barnstead tubular furnace (model 21100) and held at a constant temperature for a minimum of 1 h and a maximum of 48 h prior to each measurement. The alternating current (ac) impedance (Solartron Electrochemical Impedance Spectroscopy; SI model no. 1260, 100 mV; 0.01Hz to 7 MHz) was used to determine the conductivity. A two-probe electrochemical cell was employed for the electrical characterization. The conductivity of $\text{Sr}_3\text{NiNb}_2\text{O}_9$ was measured by subsequent heating and cooling cycles. Software Equivalent circuit Zview 4.a was used to analysis the AC impedance data.

3. Results and discussion

3.1 Structural Characterization

Fig.1 confirms the formation of perovskite-related structure for $\text{Sr}_3\text{Ni}_{1+x}\text{Nb}_{2-x}\text{O}_{9-\delta}$ ($0 \leq x \leq 1$) (SNNO) with trace of impurity. The observed peaks can be indexed on hexagonal cell constant. Also, we found a few very weak intensity (less than 5 %) peaks due to NiO (JCPDS Card No. 47-1049). The peaks (Figure 1) match with $\text{Sr}(\text{Ni}_{0.33}\text{Nb}_{0.67})\text{O}_3$ diffraction pattern and confirm the formation of perovskite related structure. Table I lists the lattice constant of SNNO.

Table 1. The lattice constant of SNNO

| Compound | Lattice constant | | |
|---|------------------|-----------|----------|
| | <i>a</i> | <i>b</i> | <i>c</i> |
| $\text{Sr}_3\text{NiNb}_2\text{O}_9$ | 5.622(2) | 5.622(2) | 6.855(3) |
| $\text{Sr}_3\text{Ni}_{1.25}\text{Nb}_{1.75}\text{O}_9$ | 5.628(12) | 5.628(12) | 6.893(1) |

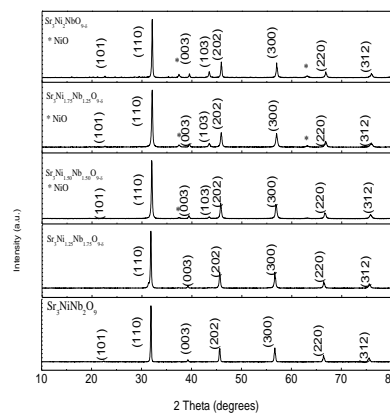


Fig.1. Powder x-ray diffraction patterns of $\text{Sr}_3\text{Ni}_{1+x}\text{Nb}_{2-x}\text{O}_{9-\delta}$ ($0 \leq x \leq 1$) (SNNO) prepared at 1000°C . Very weak impurity peaks due to NiO (JCPDS Card No. 47-1049) was observed. These impurity peaks decrease with decreasing Ni content in SNNO.

3.2 AC Impedance Spectroscopy

Fig.2 (a) and (b) show the typical impedance plots of SNNO at 525°C in ambient air, dry H_2 and wet H_2 respectively. The appearance of spike at 1 MHz value, quite visible especially at high temperature, is due to artifact of the equipment. It is also important to point out that this artifact was found to vary with total impedance of the system. For a very high total impedance system, it was found to be negligibly small. For the investigated SNNO samples, we found that the impedance plots were highly reproducible during the two subsequent heating and cooling cycles. The contributions due to bulk (b), grain-boundary (gb), and electrode (e) effects were observed at high, intermediate and low-frequency regions, especially at low temperatures. These values are typical for the bulk and grain-boundary contributions in ionic conducting ceramic materials.

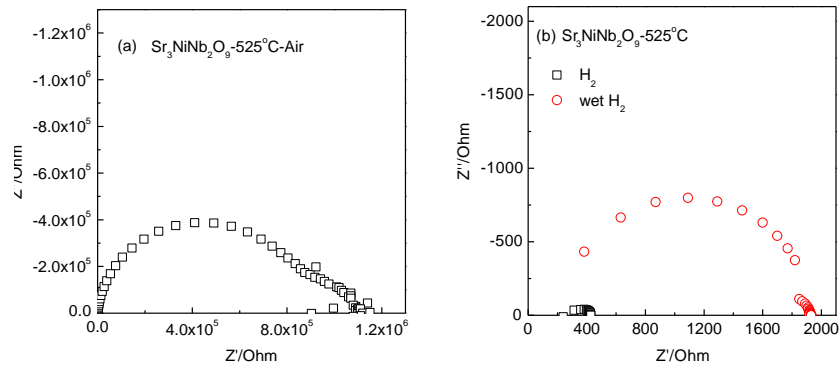


Fig.2. The typical impedance plots of SNNO at 525 °C in ambient air
(a) and (b) dry H₂ and wet H₂ respectively.

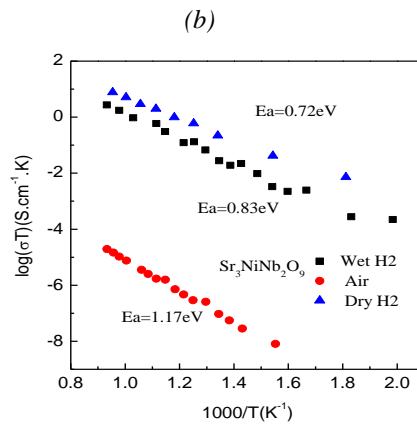


Fig.3: Arrhenius plots for total and bulk electrical conductivity of SNNO in air and wet H₂ determined by 2-probe AC electrical measurements using Pt electrodes.

The spectra show somewhat depressed arcs. It is commonly accepted that the electrode roughness and / non-homogenous distribution of physical properties cause the non-ideal behaviour. A clear intercept at the real axis at low frequencies indicates the non-blocking of the electrode and electrolyte interface, which is ascribed to absence of capacitance at the electrode and electrolyte interfaces. The low frequency intercept was considered as total impedance which includes bulk, grain-boundary and electrode effects. However, we were not able to resolve meaningfully these contributions successfully over the entire temperature range investigated, and also in various atmospheres because of strong overlap of the semicircles. In order to understand the chemical composition-structure-electrical conductivity relationship of SNNO, we uniformly took the low-frequency intercept or maximum to the real axis to determine the conductivity in all the investigated conditions. Also, for a practical application the magnitude of total conductivity is more relevant compared to those of the bulk and grain-boundary contributions.

3.3 Total Electrical Conductivity of SNNO

The Arrhenius plots for total electrical conductivity of CMO in air, dry H₂ and wet H₂ are shown in Fig.3. The electrical conductivity obtained during the heating and cooling cycles follow a

same line (Fig.4). SNNO exhibit slightly higher electrical conductivity in wet H₂ compared to dry H₂.

Table 2. the conductivity value and the activation energy of SNNO in different atmospheres

| Sr ₃ NiNb ₂ O ₉ | σ (S. cm ⁻¹) | | E_a (eV) |
|--|---------------------------------|-----------------------|------------|
| | 475°C | 675°C | |
| Air | 9.39×10^{-8} | 3.57×10^{-6} | 1.17 |
| H ₂ | 2.96×10^{-4} | 3.11×10^{-3} | 0.72 |
| Wet H ₂ | 3.73×10^{-5} | 9.81×10^{-4} | 0.83 |

As anticipated, the electrical conductivity in dry and wet H₂ was found to be much higher compared to that of in air (Fig.3). The conductivity data obtained during the first cooling and subsequent cycles follow the same line in both dry and wet H₂. In Table II, we give the conductivity value (σ) and the activation energy (E_a) for electrical conduction in different atmospheres of the investigated SNNO. The electrical conductivity in H₂ increases with decreasing in activation energy.

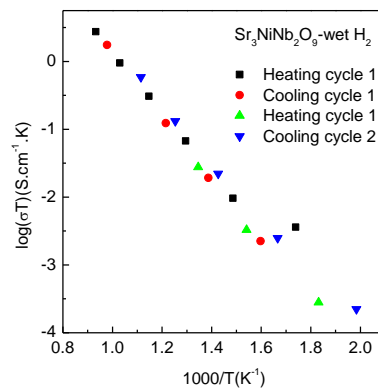


Fig.4: The electrical conductivity data for SNNO in wet H₂ obtained from the different heating and cooling cycles showed the same line, suggesting excellent reproducibility.

4. Conclusions

In summary, the formation of perovskite-related compound with a nominal chemical formula of Sr₃Ni_{1+x}Nb_{2-x}O₉ (0 ≤ x ≤ 1) (SNNO) with trace impurities were confirmed using the powder X-ray diffraction (PXRD). AC impedance measurements showed that the electrical conductivity of the Sr₃NiNb₂O₉ compound was found to vary in different atmospheres. About three to four orders of higher electrical conductivity was observed in dry and wet H₂. However, the conductivity was still low for practical application and it needs to be improved. Further work on the SNNO samples was in progress to optimize the electrical conductivity.

Acknowledgement

This research was supported by Educational Commission of Heilongjiang Province of China (No.12531117).

References

- [1] L. Carrette, K. A. Friedrich, U. Stimming, *Fuel Cells*, **1**, 5 (2001).
- [2] N. Maffei, L. Pelletier, J. P. Charland, A. Mcfarlan, *Fuel Cells* **7**, 323 (2007).
- [3] A. Lashtabeg, S. J. Skinner, *J. Mater. Chem.* **16**, 3161 (2006).
- [4] A. Boudghene Stambouli, E. Traversa, *Renewable and Sustainable Energy Reviews* **6**, 433 (2002).
- [5] R. Mark Ormerod, *Chem. Soc. Rev.* **32**, 17 (2003).
- [6] J. P. P. Huijsmans, *Current Opinion in Solid State and Materials Science* **5**, 317 (2001).
- [7] K. C. Wincewicz, J. S. Copper, *J. Power Sources* **140**, 280 (2005).
- [8] G. Korotcenkov, *Materials Science and Engineering B* **139**, 1 (2007).
- [9] N. Q. Minh, *Solid State Ionics* **174**, 271 (2004).
- [10] R. M. Ormerod, *Chem. Soc. Rev.* **32**, 17 (2003).
- [11] A. Lashtabeg, S. J. Skinner, *J. Mater. Chem.* **16**, 3161 (2006).
- [12] K. C. Wincewicz, J. S. Copper, *J. Power Sources* **140**, 280 (2005).
- [13] H. Koide, Y. Someya, T. Yoshida, T. Maruyama, *Solid State Ionics* **132**, 253 (2000).
- [14] C. W. Sun, U. Stimming, *J. Power Sources*, **171**, 247 (2007).
- [15] A. B. Stambouli, E. Traversa, *Renewable and Sustainable Energy Reviews* **6**, 433 (2002).
- [16] D. J. L. Brett, A. Atkinson, N. P. Brandon, S. J. Skinner, *Chem. Soc. Rev.* **37**, 1568 (2008).
- [17] F. Lei, B. Yan, *J. Am. Ceram. Soc.*, **92**, 1262 (2009).
- [18] Y. H. Huang, R. I. Dass, Z. L. Xing, J. B. Goodenough, *Science*, **312**, 254 (2006).